FOLIA GEOGRAPHICA • ISSN 1336-6157 (hard copy) • ISSN 2454-1001 (online)

ANALYSIS OF THE 19 JUNE 2016 SUPERCELL STORM OVER TÂRGU MUREȘ CITY, ROMÂNIA

Ion BUGLEA [A*], **Marius CIGHER** [B]

Received: June 3, 2021 | Revised: September 7, 2021 | Accepted: October 2, 2021
Paper No. 21-63/2-599

Abstract
One of the most complex mesoscale atmospheric phenomena is the supercell. In most cases it is associated with violent convective processes such as: wind intensifications that can exceed 100 km/h, high electrical activity, large hail and torrential rains in short periods of time. Such an extremely severe convective phenomenon occurred on June 19, 2016, over the city of Târgu Mureș, being the subject of this analysis. For the analysis of synoptic and mesoscale phenomena were consulted: ground and altitude maps of Global Forecast System (GFS) models, European Center for Mid-Range Weather Forecasts (ECMWF), Zentraanstalt fur Meterologie und Geodynamik (ZAMG), COSMO, ESTOFEX , Târgu Mureș Skew - T diagram, observation data from the local meteorological station, satellite images (Meteosat 08) and meteorological data from the archive of the National Meteorological Administration (ANM) and images captured by the WSR 98D Bobohalma meteorological radar. The aim of this study is to identify aspects of the structure, evolution and movement of the supercell in order to understand the synoptic and mesoscale conditions to identify the characteristic features of severe phenomena that could contribute to the effectiveness of nowcasting warnings.

Key words
Supercell, mesoscale convective system, Skew-T, low level jet, hail.

INTRODUCTION

At the base of an extreme weather situation that lasted five days was a rapidly developing cyclone. The low pressure center was formed in the Czech Republic on June 17, 2016. This center moved north and merged with the present air masses and by June 18, they formed a deep cyclone with an air pressure of 990 hPa. Further, the temperature difference between the Balkans and Central Europe increased, leading to a high horizontal temperature gradient. While in Bulgaria and Greece the pressure level was close to 25° C at an altitude of 850 hPa (about 1,500 m), above Romania it was only 10° C at the same altitude. The advection of the warm African air, which was heading north, gradually cooled, thus becoming saturated,

A* University of Oradea, 1 Universitatii Street, 410087 Oradea, Romania
https://orcid.org/0000-0002-5407-3008
bugle9@hotmail.com (corresponding author)

B Dimitrie Cantemir University, 3-5 Bodoni Sandor Street, 540545 Târgu Mureș, Romania
https://orcid.org/0000-0002-2702-7874
cighermarius@yahoo.com

providing a sufficient amount of atmospheric convection for the formation of storms. In addition to thermal parameters, an important role was played by the high altitude wind (Jetstream), and even on June 20, the altitude flow over our area was strong at the pressure level of 300 hPa (approx. 9600 m). All this created optimal conditions for thunderstorms and since the front zone has survived for a long time, along it for several days thunderstorms followed one another. The knowledge of their local climatology is not only important for weather forecasting purposes, but also for risk assessment. (Trapp et al. 2007; Kapsch et al. 2012; Allen et al. 2014; Seeley and Romps 2015; Gensini and Mote 2015; Allen 2018). Research on future climate change predicts the intensification of extreme weather events in the coming decades (Thom and Seidl, 2015). In Europe, tornadoes are rare (Dessens & Snow, 1993) and there are few studies that would associate European tornadoes with supercellular storms (Alberoni et al., 1996).

From this it can be concluded that European supercellular storms are not usually tornadoes and are much rarer than on the American continent. In central Europe thunderstorm activity peaks during summertime with a rapid increase in April and a decrease in October (Taszarek et al. 2015). Several modeling studies have been used to examine the process of supercell formation. These long-lived organized storms, first termed „supercells" by Browning (1962), have been studied extensively using radar observations and, while many characteristics are associated with supercells, the main feature that differentiates them from other thunderstorm modes is their deep, persistent, rotating updraft (Thompson 1998; Doswell and Burgess 1993). A series of studies have looked at the predictability of large-scale weather features, examining the error growth of the geopotential height forecasts at a specified pressure level (Lorenz 1982; Dalcher and Kalnay 1987; Molteni and Palmer 1993; Bengtsson and Hodges 2006).

On the other hand (Warner et al. 1984; Anthes et al. 1985; Zhang et al. 2003, 2006, 2007), have focused on the predictability on the mesoscale and a significant part dealt with the predictability of the climate and its characteristics (Kirtman 2003; Chen and Cane 2008). Only a few studies have been conducted on the predictability of the weather on the storm scale, where complex movements and turbulence occur. Studies have shown that two mechanisms are needed to form supercells in a dry environment: first, a strong flow prevents the movement of a cold exit before a storm (Klemp 1987) and second, lifting pressure gradients induce an increase in ascending current almost directly above a surface burst front (Schlesinger 1980; Rotunno and Klemp 1982).

Following studies on the environment around supercells, (Weisman and Klemp 1982) concluded that supercell formation is more favorable in environments with high instability and strong vertical wind. In Romania, the appearance of supercells is very rare, but the case of the severe meteorological phenomenon from 19.06.2016 in the Târgu Mureș area, studied in this paper suggests that such events will be more frequent in the next period. This case study analyzes the synoptic and mesoscale conditions that determined the formation of the supercell. This article is structured as follows: Section 2 describes the data sets and methodology, section 3 presents in subsections (synoptic situation, mesoscale situation, analysis of satellite images, analysis of electric discharges and precipitation, analysis of the aerological diagram and instability indices, radar data analysis), The conclusions are presented in section 4.

DATA AND METHODS

To perform this analysis were used the database of the National Meteorological Administration (ANM) archive on air temperature, pressure, humidity, amount of precipitation, meteorological phenomena with hourly and daily meteorological measurements. At the synoptic level, maps of the ground level and the baric and thermal field at different altitudes 500 and 850 hPa were analyzed from http://www1.wetter3.de/archiv_gfs_en.html.

To examine the vertical structure of the supercell, the infrared images captured by the meteorological satellite Meteosat 08 were analyzed, (ANM Archive). The horizontal evolution was analyzed using the data from the S band of the Doppler radar WSR-98D Bobohalma (RDBB) from June 19, (ANM Archive), with a coverage area of 166106 square km radius of 230 km, reflexivity field at 2.4 degree elevation, with a periodic scan of 6 minutes. The main studied parameters of convective cells were the height of cloud formations (Echo Tops), reflectivity and vertically integrated liquid (VIL), hail indices (Hail Index). The radar analysis was supplemented by data provided by the European lightning detection network Blitzortung, (https://www.blitzortung.org/en/historical_maps.php?map=10) and the radiosonde measurements were acquired following the analysis of the COSMO model.

RESULTS AND DISCUSSION

a) Synoptic situation

Synoptic map of Europe (Fig. 1), on 19.06.2016 shows the Azoric anticyclone with a central pressure of 1033 hPa, in the western half of Europe, with the ridge extended to the northeast of the continent, carrying maritime subpolar air, coupled with the depression area of North Atlantic origin centered in Finland, simultaneously with the advection of hot and humid air extended over central Europe. The studied area is located in the separation surface between the two air masses highlighted by the high potential equivalent temperature gradient. The flow of hot and humid air from the Mediterranean Sea was the triggering synoptic ingredient that led to the formation of increased atmospheric instability on 19.06.2016. Following this synoptic context, the supercellular storm was formed, manifested by abundant precipitation, strong wind and large hail, a very rare meteorological phenomenon in the studied area that can occur once every 10 years.

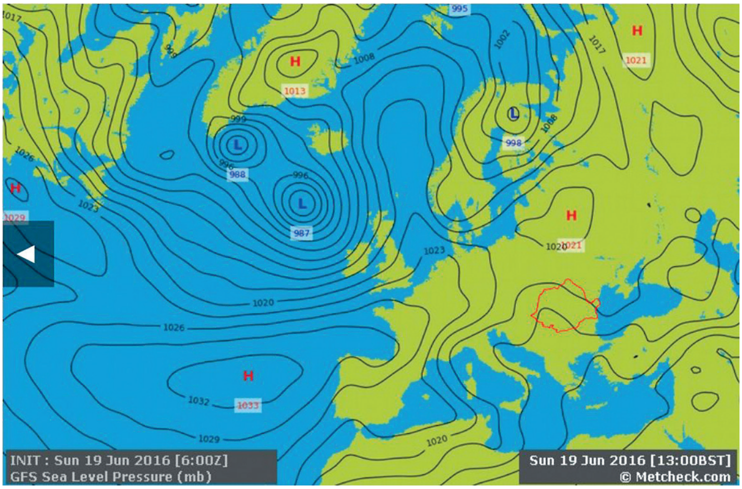

Fig. 1
Synoptic map of Europe pressure on 19.06.2016, 13:00 BST, GFS model analysis
Source: (https://www.metcheck.com/WEATHER/gfscharts_archive.asp)

b) Mesoscale situation

At an altitude of 500 hPa, on June 19, the geopotential map of Europe shows the ridge of North African origin in the southeast of the continent with geopotential values of 584 dmgp. The instability is accentuated on the tropospheric column due to the extension of the Icelandic cyclone trough to the central basin of the Mediterranean Sea presented by a cut-off structure of 568 dmgp (Fig. 2-a).

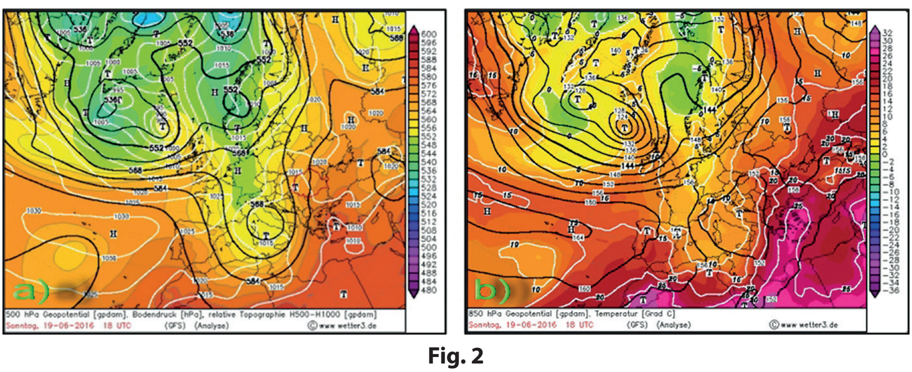

Fig. 2
GFS model analysis for Europa at 19.06.2016, 18:00 UTC,
a) Geopotential map at level of 500 hPa, b) Temperature map at level of 850 hPa.
Source:(http://www1.wetter3.de/archiv_gfs_en.html)

The area of interest is located on the ascending slope of the plateau, inside the contact surface between the cold and humid air mass penetrated from the west due to the Azores anticyclone on the ground, the hot and dry air mass at altitude, present in south-eastern Europe. cold air mass due to the altitude trough detached from the Icelandic cyclone. In this synoptic context within the discontinuity line, the thermo-baric gradient intensified being favored by the moist air mass transported by the ridge of the Azores anticyclone, finally conditioning the formation of the studied supercell. According to the GFS model, the values of the equipotential temperature at the level of 850 hPa, on June 19, at 18:00 UTC, are determined by the advection of a warm air mass from North Africa of 25° C, loaded with moisture over the Mediterranean Sea, associated with the valley. of the Icelandic cyclone of 10° C, which transports cold air, doubled by the Azoric anticyclone through the ridge extended to southeastern Europe (Fig. 2-b). This area is highlighted by the potentially high equivalent temperature gradient being oriented from northeast to southwest, starting with southern Ukraine, western Romania, Serbia and southern Italy.

At the level of 300 hPa, in the upper troposphere, from the analyzes of the ALARO numerical model, there is an extended warm ridge with a geopotential value of 952 dmg in the area of interest, having a slight increase of the gradient value in the geopotential field up to 954 dmg at 18:00 UTC. In the thermal field the temperature increased by about 2° C, these conditions ensuring a surplus of ascendancy to the convective phenomena in this area. This configuration of association of the lower level jet with the jet from the upper troposphere favors the development and maintenance of the activity of convective cells (Blaga, 2015).

c) Analysis of satellite images

The infrared image captured by Meteosat 08 illustrates the accentuated vertical development of cloud formations, the estimated temperature at the top of cloud systems being approximately (- 65° C), (Fig. 3-a) on June 19, 2016 at 17:00 UTC.

To monitor the tendency of the convective system to move, the High Resolution Visible (HRV) images from 17:20 UTC were analyzed, from where the trajectory of the mesoscale convective system can be observed, which was from SW to NE, as well as its evolution along the route, where the most developed cells had a cloudy roof of 10-12 km. In the image (Fig. 3-b) the green arrow indicates the overshooting of the analyzed supercell that has climbed up to 15 km, and the blue star indicates the position of the studied area.

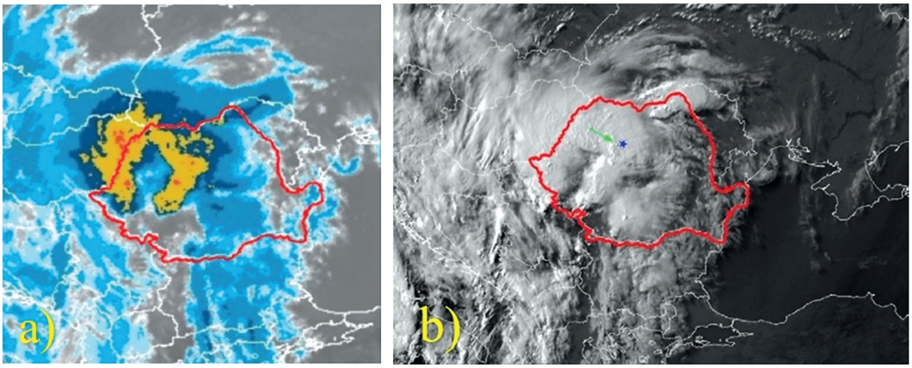

Fig. 3
Images provided by Meteosat 08,
a) infrared at 17:00 UTC, b) High Resolution Visible (HRV) at 17:20 UTC.
Source: (ANM Archive)

d) Analysis of electric discharges and precipitation

A method for monitoring thunderstorm activity is by remote sensing, such as lightning detection networks. A number of thunderstorm climatologies have been based on lightning detection networks at national, continental, or global scales (Betz et al. 2009; Pohjola and Mäkelä 2013; Virts et al.2013; Wu et al. 2016;Galanaki et al. 2018; Zhang et al.2018). The electrical activity was intense throughout the trajectory of the convective cells, but the peak was recorded between 17:00 - 17:30 UTC, very close to the studied area (Fig. 4-a).

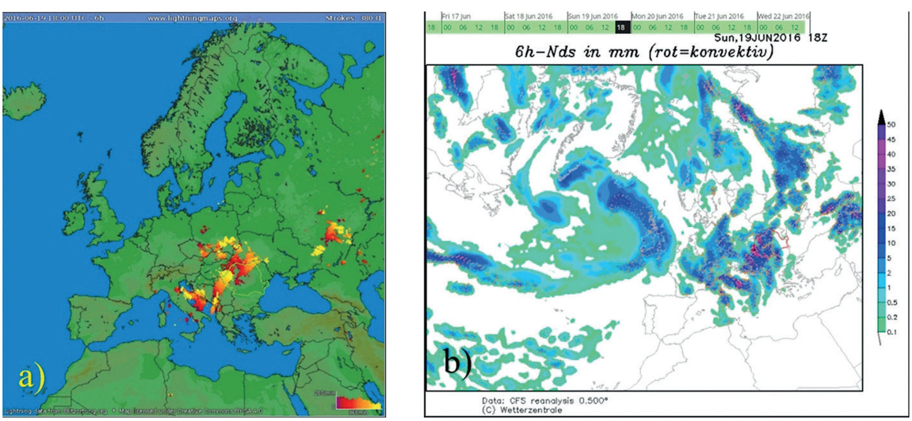

Fig. 4
GFS model analysis for Europa at 19.06.2016, 18:00 UTC,
a) Lightning distribution. *Source: (https://www.blitzortung.org/en/historical_maps.php?map=10),*
b) Precipitation area. *Source: (https://www.wetterzentrale.de/reanalysis.php?jaar=2016&maand=6&dag=19&uur=1800&var=4&map=1&model=cfsr)*

The synoptic situation presents a convective system with a particularly fast evolution (Fig. 4-b), with an accentuated atmospheric instability, which had supercellular characteristics, associated with torrential rains that locally exceeded 40-50 l/square meters and medium-sized hail. Convective storms had the trajectory of movement from SW to NE.

e) Analysis of the aerological diagram and instability indices

June 19 brought together all the synoptic ingredients needed to trigger extreme phenomena specific to increased atmospheric instability. The instability on the entire tropospheric column is due to the interaction of the Icelandic Cyclone basin extended to the center of the Mediterranean Sea and the North African ridge in southeastern Europe of the Azoric anticyclone. The COSMO limited area model presents for the area of interest indices of instability in the altitude survey on 19.06.2016, with the following values: Total Totals Index (TTI) values increased to 55-57, indicating the possibility of tornadoes, values Convective Available Potential Energy (CAPE), were over 2100 J/kg indicating pronounced instability, Lifted Index (LI) values, decreased to - 7° C, values associated with extreme instability and extreme large storms, K Index values (KI) reached 38-40, indicating a probability of 80-89% storm. The Skew-T aerological diagram, dated 19.06.2016, at 18:00 UTC (Fig. 5), shows the visualization of the basic transformations of atmospheric energy by the vertical evolution in the Earth's atmosphere of the dew point curve (left), of humidity (middle) and temperature (right). The difference between the temperature graph curve and the dew point graph indicates the value of air mass humidity, level by level. The smaller the space, the more humid the air. If the curves overlap, they correspond to 100% saturated air and condition the appearance of clouds (Fig. 5a). The graph shows on the left the standard pressure levels defined by the International Civil Aviation Organization (ICAO) and on the right is the force and direction of the wind, a half barb corresponds to 5 knots or 10 km/h, 1 barb corresponds to 10 knots or 20 km/h and a triangle to 50 knots or 100 km/h. The graph shows the vertical shear of the wind below 1500 m, this being an indicator of the formation of convective storms. This figure represents a COSMO environmental sounding model, together with the equivalent hodograph in the upper right corner (Fig. 5b), representing the wind speed and direction as well as the shear, in relation to the height. At the same time, there is a dry layer at low levels below 1500 m, a wet layer at medium levels and a drier range between 500 and 400 hPa levels, which favor the instability of the atmosphere. The isotherm of 0 degrees at 3500 m, is an exact indicator for the appearance of medium and large hail, which in association with the CAPE index with extremely high values, favored the maintenance of ice particles inside the cloud for a long time, resulting in large hail.

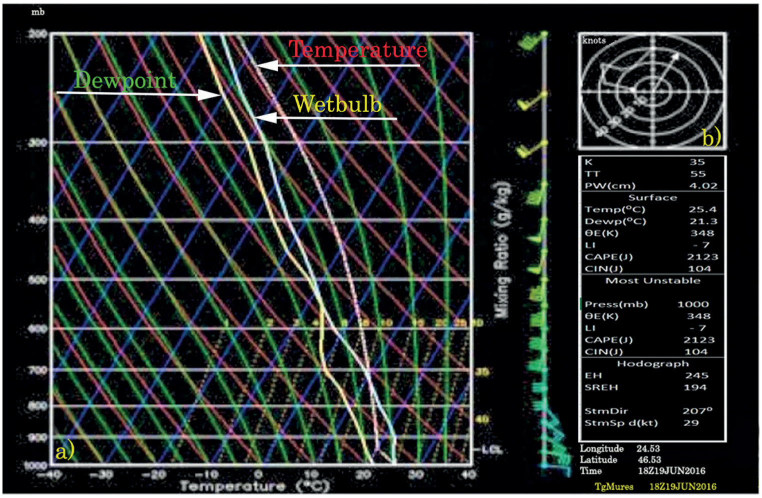

Fig. 5
COSMO model analysis Skew T diagram for Târgu Mureș at 19.06.2016, 18:00 UTC
a) environmental sounding model, b) hodograph
Source: (ANM archive)

f) Radar data analysis

Climatological aspects of (severe) thunderstorms can also be studied using national radar networks (Davini et al. 2011; Cintineo et al. 2012; Kaltenböck and Steinheimer 2015). From a convective point of view, June was very active, especially in the second half of the month when violent storms occurred in most areas of the country due to intense cyclogenesis in central and northwestern Europe, due to the contrast between the cold air mass in the central part and the advection of warm air in Eastern Europe, favored by the ridge of the Azoric anticyclone. In the early stages, convective phenomena manifested themselves in the west of the country, where supercellular systems could be observed. These turned into convective systems (arc echoes) that eventually formed a storm line. The trajectory of a mesoscale convective system is usually with lines of thickness 300-850 hPa or in general the movement of convective cells in a convective system is deflected to the right of the wind from average levels by about 30° and at a speed lower than this, on average 70% (Merritt and Fritsch, 1984).

Initially, the cells of the mesoscale convective system had a southwest-northeast trajectory and then a slight eastward rotation. The supercell was detected at 16:20 UTC, at a distance of over 90 km west of the S-band Doppler WSR-98D radar from Bobohalma meteorological radar (RDBB), and traveled approximately 145 km, with an average speed of 50 km/h and a lifespan of almost 3 hours. In the reflexivity field at an elevation of 2.4 degrees, at 17:16 UTC, (Fig. 6), the mesoscale convective system is in the maximum development phase, presenting values of 70 dBz and takes the form of an arched echo. The white circle indicates the study area.

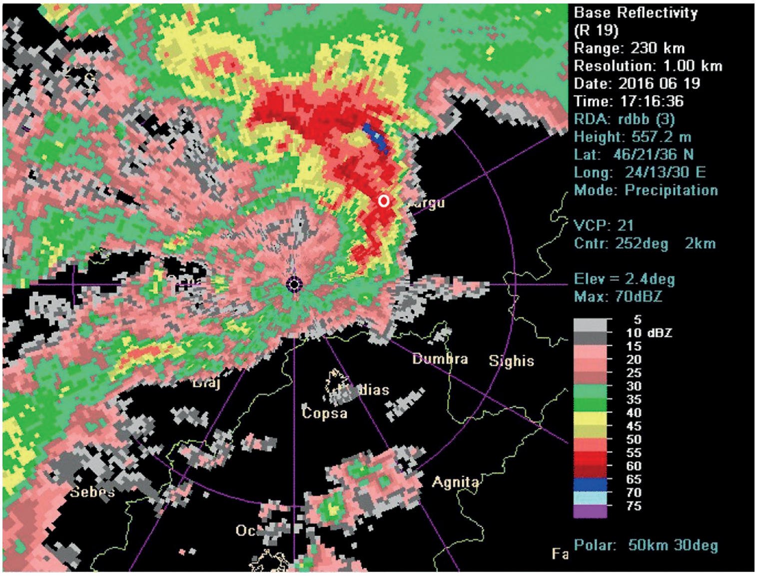

Fig. 6
Reflexivity field at 2.4 degree elevation, 19.06.2016, 17:16 UTC,
Bobohalma meteorological radar (RDBB).
Source: (ANM Archive)

Fig. 7
Supercell at the city limit.

Reflectivities larger than 55 dBZ are often attributed to hail (Geotis, S.G., 1963). The radar data were also confirmed by the measurements made at the local meteorological station, where the amount of precipitation reached 40 l/square meters, hail with a diameter of 2-3 cm fell and the wind gusts reached 70 km/h. For România, Carbunaru (2014) and Reckerth (2015) correlated some radiolocation parameters of Cumulonimbus clouds which produced hail falls. Figure 7 shows the magnitude of the phenomenon just before it hit the city.

CONCLUSIONS

Thunderstorms, particularly severe events accompanied by large hail, damaging wind gusts, tornadoes, or flash floods, pose a considerable risk to society (Brooks 2013; Papagiannaki et al. 2013; Terti et al. 2017; Papagiannaki et al. 2017). Between June 18-20, 2016, in the southern and central-eastern part of Europe, supercellular structures and the extreme meteorological phenomena associated with them were reported. For such an extreme phenomenon to form, a combination of factors is needed. On June 19, 2016 all the conditions necessary for the formation of a storm of such intensity were met in the area of Târgu Mureș. We cannot say that it was a tornado, but according to the analysis regarding the damage produced, it was concluded that there was an extremely violent downburst with an estimated wind speed of 150 km/h. Recently research on the phenomenon has intensified in order to understand and be able to explain their properties (Solari, 2014, 2020).

At ground level, conditions were formed for the overlap of the hot and dry air mass stationed on the Romanian territory, with the mass of cold and humid air through the western advection of the Azores anticyclone ridge. In altitude, the geopotential gradient increased following the interaction exerted by the Azores ridge located in the southeast of the country and the Icelandic depression, amplifying the descent of cold air. The western half of the country was in the area of interference between the two air masses. The advancement of hot and humid air provided by the low level jet played a decisive role in increasing the instability and the potential of severe weather. It is unusual for such extreme storms to persist in our region for several days.

If the potential energy of a convective system is provided by surface heating caused by solar radiation, it will take several hours, but if the potential energy supply is made at the synoptic scale, by humidity in the middle troposphere, continuous flow of cold air in the upper troposphere, associated with wind shear, then the lifespan can be extended to a few days, as in this case. The evolution of the studied supercell reached its peak on the afternoon of June 19th. This study tried to identify the causes and processes that favored the evolution of convective systems between June 18-20, but especially the case of the supercellular system and the storm line of June 19 in Târgu Mureș area, to improve the methods of issuing warnings in case such extreme phenomena, which in the future will be more numerous.

REFERENCES

ALBERONI, P.P., NANNI, S., CRESPI, M. & MONAI, M. (1996). The supercell thunderstorm on 8 June 1990, Mesoscale analysis and radar observations. *Meteorol. and Atmos Phys.*, 58:123-138.

ALLEN, J. T., AND D. J. KAROLY, (2014). A climatology of Australian severe thunderstorm environments 1979–2011: Inter-annual variability and ENSO influence. *Int. J. Climatol*., 34, 81–97, https://doi.org/10.1002/joc.3667.

ALLEN, J. T., (2018). Climate change and severe thunderstorms. *Oxford Research Encyclopedia of Climate Science*, Oxford University Press, https://doi.org/10.1093/acrefore/9780190228620.013.62.

ANTHES, R. A., Y. H. KUO, D. P. BAUMHEFNER, R. M. ERRICO, AND T. W. BETTGE, (1985). Predictability of mesoscale atmospheric motions. *Adv. Geophys*., 28B, 159–202.

BENGTSSON, L., AND K. I. HODGES, (2006). *A note on atmospheric predictability*. Tellus, 58A, 154–157.

BETZ, H. D., K. SCHMIDT, P. LAROCHE, P. BLANCHET, W. P. OETTINGER, E. DEFER, Z. DZIEWIT, AND J. KONARSKI, (2009). LINET An international lightning detection network in Europe. *Atmos. Res*.,91, 564–573, https://doi.org/10.1016/j.atmosres.2008.06.012.

BLAGA, IRINA. (2015). Cantităţi însemnate de precipitaţii în judeţul Cluj. Factori favorizanţi, în *revista Ştiinţifică a Administraţiei Naţionale de Meteorologie*, Bucureşti ISSN:2069-878X, ISSN-L=2069-878X,http://www.meteoromania.ro/images/raport/revistastiintifica2015.pdf.

BROWNING, K. A., (1962). Cellular structure of convective storms. *Meteor. Mag*., 91, 341–350.

BROOKS, H. E., (2013). Severe thunderstorms and climate change. *Atmos. Res*.,123, 129–138, https://doi.org/10.1016/j.atmosres.2012.04.002.

CARBUNARU, D., (2014). Detection of hail through the three-body scattering signatures and its effects on radar algorithms observed in Romania, *Atmósfera* 27(1), 21-34, DOI:10.1016/S0187-6236(14)71098-7.

CHEN, D., AND M. A. CANE, (2008). El Ni~no prediction and predictability. *J. Comput. Phys*., 227, 3625–3640.

CINTINEO, J. L., T. M. SMITH, V. LAKSHMANAN, H. E. BROOKS, AND K. L. ORTEGA, (2012). An objective high-resolution hail climatology of the contiguous United States. *Wea. Forecasting*, 27,1235–1248, https://doi.org/10.1175/WAF-D-11-00151.1.

DAVINI, P., R. BECHINI, R. CREMONINI, AND C. CASSARDO, (2011). Radar-based analysis of convective storms over northwestern Italy. *Atmosphere*, 3, 33–58, https://doi.org/10.3390/atmos3010033.

DALCHER, A., AND E. KALNAY, (1987). *Error growth and predictability in operational ECMWF forecasts*. Tellus, 39, 474–491.

DESSENS, J. & SNOW, J.T. (1993). *Comparative description of tornadoes in France and the United States.* Geophys. Monogr., 79: Am. Geophys. Union, 427-434.

DOSWELL, C. A., AND D. W. BURGESS, (1993). Tornadoes and tornadic storms. A review of conceptual models. The Tornado: Its Structure, Dynamics, Hazards, and Prediction,Geophys. Monogr., Vol. 79, *Amer. Geophys. Union*, 161–172.

GALANAKI, E., K. LAGOUVARDOS, V. KOTRONI, E. FLAOUNAS, AND A. ARGIRIOU, (2018). Thunderstorm climatology in the Mediterranean using cloud-to-ground lightning observations. *Atmos. Res*., 207, 136–144, https://doi.org/10.1016/j.atmosres.2018.03.004.

GENSINI, V. A., AND T. L. MOTE, (2015). Downscaled estimates of late 21st century severe weather from CCSM3. *Climatic Change*, 129, 307–321, https://doi.org/10.1007/s10584-014-1320-z.

GEOTIS, S.G. (1963). Some radar measurements of hailstorms. *J. Appl. Meteorol*., 2: 270-275.

KALTENBÖCK, R., ANDM. STEINHEIMER, (2015). Radar-based severe storm climatology for Austrian complex orography related to vertical wind shear and atmospheric instability. *Atmos. Res*., 158–159,216–230, https://doi.org/10.1016/j.atmosres.2014.08.006.

KAPSCH, M. L., M. KUNZ, R. VITOLO, AND T. ECONOMOU, (2012). Long-term trends of hail-related weather types in an ensemble of regional climate models using a Bayesian approach. *J. Geophys. Res*., 117, D15107, https://doi.org/10.1029/2011JD017185.

KIRTMAN, B. P., (2003). The COLA anomaly coupled model: Ensemble ENSO prediction. *Mon. Wea. Rev*., 131, 2324–2341.

KLEMP, J. B., (1987). Dynamics of tornadic thunderstorms. *Annu. Rev. Fluid Mech*., 19**,** 369–402.

LORENZ, E. N., (1982). *Atmospheric predictability experiments with a large numerical model. Tellus*, 34, 505–513.

MERRITT, J. H., AND J. M. FRITSCH, (1984). On the movement of the heavy precipitation areas of mid-latitude mesoscale convective complexes. Preprints, 10th *Conference on Weather Forecasting and Analysis*, Tampa, Fla., American Meteorological Society, Boston.

MOLTENI, F., AND T. N. PALMER, (1993). Predictability and finite-time instability of the northern winter circulation. *Quart. J. Roy. Meteor. Soc*., 119, 269–298.

PAPAGIANNAKI, K., K. LAGOUVARDOS, AND V.KOTRONI, (2013). A database of high-impact weather events in Greece: A descriptive impact analysis for the period 2001–2011. *Nat. Hazards Earth Syst. Sci*., 13, 727–736, https://doi.org/10.5194/nhess-13-727-2013.

PAPAGIANNAKI, K., V. KOTRONI, K. LAGOUVARDOS, I. RUIN, AND A. BEZES, (2017). Urban area response to flash flood–triggering rainfall, featuring human behavioral factors: The case of 22 October 2015 in Attica, Greece. *Wea. Climate Soc.*, 9, 621–638, https://doi.org/10.1175/WCAS-D-16-0068.1.

POHJOLA, H., A. MÄKELÄ, (2013). The comparison of GLD360 and EUCLID lightning location systems in Europe. *Atmos. Res.*, 123, 117–128, https://doi.org/10.1016/j.atmosres.2012.10.019.

RECKERTH U. D., (2015). Correlations between hail events and radar echoes in Transylvania., *Aerul și Apa. Componente ale Mediului* pp.413–420, DOI: 10.17378/AWC2015_54.

ROTUNNO, R., AND J. B. KLEMP, (1982). The influence of the shear shearinduced pressure gradient on thunderstorm motion. *Mon. Wea. Rev.*, 110, 136–151.

SCHLESINGER, R. E., (1980). A three-dimensional numerical model of an isolated thunderstorm. Part II: Dynamics of updraft splitting and mesovortex couplet evolution. *J. Atmos. Sci.*, 37, 395–420.

SEELEY, J. T., AND D. M. ROMPS, (2015). The effect of global warming on severe thunderstorms in the United States. *J. Climate*, 28, 2443–2458, https://doi.org/10.1175/JCLI-D-14-00382.1.

SOLARI, G., (2014). Emerging issues and new frameworks for wind loading on structures in mixed climates. *Wind Struct*. 19, 295–320.

SOLARI, G., (2020). Thunderstorm downburst and wind loading of structures: progress andprospect. *Front. Built Environ*. 6 (63), 1–24.

TASZAREK, M., ALLEN, J., PÚČIK, T., GROENEMEIJER, P., CZERNECKI, B., KOLENDOWICZ, L., LAGOUVARDOS, K., KOTRONI, V., & SCHULZ, W. (2015). A Climatology of Thunderstorms across Europe from a Synthesis of Multiple Data Sources. *Journal of Climate*, 32(6), 1813-1837. Retrieved May 26, 2021, from https://journals.ametsoc.org/view/journals/clim/32/6/jcli-d-18-0372.1.xml

TERTI, G., I. RUIN, S. ANQUETIN, AND J. J. GOURLEY, (2017). A situation based analysis of flash flood fatalities in the United States. *Bull. Amer. Meteor. Soc.*, 98, 333–345, https://doi.org/10.1175/BAMS-D-15-00276.1.

THOM, D., SEIDL , R., (2015). Natural disturbance impacts on ecosystem services and biodiversity in temperate and boreal forests. *Biological Reviews*. Doi: 10.1111/brv.12193.

THOMPSON, R. L., (1998). Eta model storm-relative winds associated with tornadic and nontornadic supercells. *Wea. Forecasting*,13, 125–137.

TRAPP, R. J., N. S. DIFFENBAUGH, H. E. BROOKS, M. E. BALDWIN, E. D. ROBINSON, AND J. S. PAL, (2007). Changes in severe thunderstorm environment frequency during the 21st century caused by anthropogenically enhanced global radiative forcing. *Proc. Natl. Acad. Sci.* USA, 104, 19 719–19 723, https://doi.org/10.1073/pnas.0705494104.

VIRTS, K. S., J. M. WALLACE, M. L. HUTCHINS, AND R. H. HOLZWORTH, (2013). Highlights of a new ground-based, hourly global lightning climatology. *Bull. Amer. Meteor. Soc.*, 94, 1381–1391,https://doi.org/10.1175/BAMS-D-12-00082.1.

WARNER, T. T., D. KEYSER, AND L. W. UCCELLINI, (1984). Some practical insights into the relationship between initial state uncertainty and mesoscale predictability. *Proc. American Institute of Physics Conf*., La Jolla, CA, G. Holloway and B. West, Eds., American Institure of Physics, 271–286.

WEISMAN, M. L., AND J. B. KLEMP, (1982). The dependence of numerically simulated convective storms on vertical wind shear and buoyancy. *Mon. Wea. Rev*., 110, 504–520.

WU, F., X. CUI, D. L. ZHANG, D. LIU, AND D. ZHENG, (2016). SAFIR- 3000 lightning statistics over the Beijing metropolitan region during 2005–07. *J. Appl. Meteor*. Climatol., 55, 2613–2633, https://doi.org/10.1175/JAMC-D-16-0030.1.

ZHANG, F., C. SNYDER, AND R. ROTUNNO, (2003). Effects of moist convection onmesoscale predictability. *J. Atmos. Sci*., 60, 1173–1185.

ZHANG, F., A. M. ODINS, AND J. W. NIELSEN-GAMMON, (2006) .Mesoscale predictability of an extreme warm-season precipitation event. *Wea. Forecasting*, 21, 149–166.

ZHANG, F., N. BEI, R. ROTUNNO, C. SNYDER, AND C. C. EPIFANIO, (2007). Mesoscale predictability ofmoist baroclinicwaves:Convectionpermitting experiments and multistage error growth dynamics. *J. Atmos. Sci*., 64, 3579–3594.

ZHANG, W., Y. ZHANG, D. ZHENG, L. XU, AND W. LYU, (2018). Lightning climatology over the northwest Pacific region: An 11-year study using data from the World Wide Lightning Location Network. *Atmos. Res*., 210, 41–57, https://doi.org/10.1016/j.atmosres.2018.04.013. https://www.metcheck.com/WEATHER/gfscharts_archive.asp (accessed on March 15, 2021)

http://www1.wetter3.de/archiv_gfs_en.html (accessed on March 18, 2021)

https://www.blitzortung.org/en/historical_maps.php?map=10 (accessed on April 16, 2021)

https://www.wetterzentrale.de/reanalysis.php?jaar=2016&maand=6&dag=19&uur=1800&var=4&map=1&model=cfsr (accessed on April 16,2021)